King Saud University

Arabian Journal of Chemistry

www.ksu.edu.sa
www.sciencedirect.com

ORIGINAL ARTICLE

Synthesis, characterization, antimicrobial and cytotoxic studies of a novel vanadium dodecylamino phosphate

A. Rajini, M. Nookaraju, N. Venkatathri *, I.A.K. Reddy

Department of Chemistry, National Institute of Technology, Warangal 506 004, Andhra Pradesh, India

Abstract A novel vanadium dodecylamino phosphate was synthesized by mixing phosphoric acid and vanadyl acetylacetonate with dodecylamine at ambient temperature. The material was characterized by various spectroscopic and analytical techniques to know its morphological and structural characteristics. The biological activity of the material toward antimicrobial, nematicidal, DNA cleavage and cytotoxicity has been screened. The material exhibits moderate to good antimicrobial activity against Gram-positive bacteria. The percentage mortality on *Meloidogyne incognita* nematode was found to increase with increase in concentration of VDDAP at 48 h. Further, the material was investigated for cytotoxicity on human cancer cell lines such as cervix (HeLa), leukemia (HL60) and breast (MCF7). The cells were dosed with varying concentrations of the VDDAP and cell viability was measured by sulforhodamine B (SRB) assay to determine their GI50 values. Interestingly, the compound shows GI50 values of 25.4 $\mu g\,mL^{-1}$ (HeLa), 29.1 $\mu g\,mL^{-1}$ (MCF7) and a superior value of 11.6 $\mu g\,mL^{-1}$ (HL60) respectively. The DNA cleavage activity of the material was investigated using agarose gel electrophoresis.

© 2013 Production and hosting by Elsevier B.V. on behalf of King Saud University.

1. Introduction

The fight against cancer is the primary target concerning medicinal chemistry. *Cis*-platin and carboplatin are some of the widely used chemotherapeutic drugs. However these drugs cause strong side effects and difficulties which limit their use in medicine. Recently, non platinum group metals are found to exhibit pronounced *in vivo* and *in vitro* activities against various tumor cell lines. As platinum group metals are costly and difficult to procure at low costs, researchers look forward to the application of non platinum group metals toward anticancer studies and focused in applying various transition metals in biological applications. The metal based compounds such as vanadium, titanium, copper, ruthenium, tin and rhodium have been reported with promising chemotherapeutic potentials (Ott and Gust, 2007). Among the metal based compounds, vanadium compounds have been implicated in many biological processes like cell growth and known to possess therapeutic applications

* Corresponding author. Mobile: +91 9491319976.
E-mail address: venkatathrin@yahoo.com (N. Venkatathri).

such as anticancer (Shahzadi et al., 2010), anti-diabetic (Thompson et al., 1999) and anti-HIV properties.

Vanadium is an essential element for various biological functions and used in biochemistry and cell biology (Chasteen et al., 1983) as a tool to characterize various molecular processes. Vanadium ions can play a major role in biology as counter ions for protein, DNA, RNA and in various biological organelles. Some compounds of vanadium induce apoptosis in human leukemia, multiple myeloma and suppress the growth of existing tumors by limiting the invasion and metastatic potential of neoplastic cells (Benítez et al., 2011; Maia et al., 2009). The compounds of vanadium are capable of regulating signal transduction pathways, promote cell transformations, enzyme activities, cell-to-cell communications and adhesions (Morinville et al., 1998). Successful studies over the past few decades have advanced the use of vanadium compounds as anticancer agents in the preclinical stage for cancers of breast, colon, liver and leukemia. (Bishayee et al., 2010).

The nuclease activity of vanadium compounds was first reported in Shi et al. (1996) for $VOSO_4$ in the presence of Hydrogen peroxide. Several cationic V^{3+} dimeric complexes with 1,10-phenanthroline were shown to have nuclease activity (Heater et al., 2000). Verquin et al. (2004) synthesized V^{4+} complexes with hydroxysalen ligands which shows nuclease activity in the presence of an activating agent, either a reducing mercaptopropionic acid (MPA) or an oxidizing oxone ($KHSO_5$). In the present study, we report a novel vanadium dodecylamino phosphate prepared instantly by simple mixing of its precursors at ambient temperature. The material was characterized by various physicochemical techniques such as powder XRD, SEM-EDAX, FT-IR, Raman spectroscopy, UV–Vis DRS, ^{31}P and ^{13}C MAS NMR. As part of our study we have investigated biological activity such as antimicrobial, DNA cleavage and cytotoxicity of vanadium dodecylamino phosphate.

2. Experimental

2.1. Materials

Vanadyl acetylacetonoate (Sigma–Aldrich, India 98%), dodecylamine (Sigma–Aldrich, India 98%) and orthophosphoric acid (Merck, India 85%) were obtained. All chemicals were of analytical reagent grade and used as received without any further purification.

2.2. Synthesis of vanadium dodecylamino phosphate (VDDAP)

The synthesis of vanadium dodecylamino phosphate (VDDAP) was carried out at ambient temperature as reported elsewhere (Rajini et al., 2013). In a typical synthesis, a pre-determined quantity of orthophosphoric acid (1 M) was added to vanadyl acetylacetonoate (0.01 M) and stirred until the vanadyl acetylacetonoate was dissolved. Dodecylamine (4 M) was added to this mixture and stirred well to obtain a solid product. The product thus obtained was thoroughly washed with ether, dried at 50 °C for about 1 h and grounded to obtain VDDAP.

2.3. Characterization techniques

Qualitative phase analysis of VDDAP was performed using a Bruker AXS D8 Advance diffractometer at ambient temperature with Cu K_α X-ray source of wavelength of 1.5406 Å using a Si(Li) PSD detector. The morphology of the synthesized material was investigated using a JEOL Model JSM6390LV of scanning electron microscope (SEM) and the surface elemental composition (EDAX) was examined using a JEOL Model JED-2300. Fourier transform infrared (FT-IR) spectra were recorded on a Thermo Nicolet Avatar 370 spectrophotometer equipped with a pyroelectric detector (DTGS type) a resolution of 4 cm^{-1} was adopted, provided with a KBr beam splitter. Dispersive Raman spectroscopy was performed on a Bruker Senterra at a wavelength of 532 nm using laser radiation as the source. The coordination and the oxidation state of vanadium in VDDAP were examined by diffuse reflectance UV–Vis spectrophotometry (UV–Vis DRS) on a Varian Cary 5000 in the range of 175–800 nm. Solid state ^{31}P magic angle spinning (MAS) nuclear magnetic resonance (NMR) spectra were recorded on a Bruker DRX-500 AV-III 500(S) spectrometer. The ^{31}P MAS NMR spectrum was recorded at 121.49 MHz in the frequency range of 10–12 kHz using a 5 mm dual probe head of pulse duration of 5 μs. The chemical shift was measured with regard to 85% H_3PO_4 as the external reference. The solid state ^{13}C magic angle spinning (MAS) nuclear magnetic resonance (NMR) spectra was recorded on a DSX-300 Avance-III 400(L) NMR spectrometer. The ^{13}C MAS NMR spectrum was recorded at 75.47 MHz in the frequency range of 10–12 kHz equipped with using a 5 mm dual probe head of pulse duration 4.25 μs.

2.4. In vitro antimicrobial studies

The *in vitro* anti-bacterial and anti-fungal activities of the VDDAP were tested against Gram-positive (*Staphylococcus aureus*, *Bacillus subtilis*), Gram-negative bacteria (*Pseudomonas fluorescens*, *Escherichia coli*, and *Proteus vulgaris*) and fungal species (*Candida albicans*) by the disc diffusion method. The antibiotics ampicillin and clotrimazole are the standards for anti-bacterial and anti-fungal activity studies. Nutrient agar plate was evenly spread by using a sterile glass spreader. Sterile antibiotic discs (Whatman No. 1 paper having the diameter 6 mm) were placed over the medium. To determine the antimicrobial activity, 100 μg mL^{-1} of VDDAP initially dissolved in dimethyl sulphoxide (DMSO) was transferred to each disc with the help of a micropipette, simultaneously maintaining standard ampicillin (30 μg/disc) against bacteria and clotrimazole (10 μg/disc) for fungi. After overnight incubation at 37 °C for bacteria and 25 °C for fungi, the zone of inhibition was measured in 'mm' and compared with standard antibiotics. Control measurements were carried out with DMSO. All the experiments were performed in triplicate and the average zone of inhibition was calculated. Minimum inhibitory concentration (MIC) value of VDDAP was determined by using the serial dilution method.

2.5. Nematicidal activity

Nematicidal activity was carried out on *Meloidogyne incognita*. Nematode *M. incognita* is known to attack more than 3000 host plants (Reddy and Khan, 1991). The yields of okra, tomato and brinjal typically suffer 90.9%, 46.2% and 2.3% losses, respectively due to *M. incognita*. *M. incognita* produces galls on the roots of many host plants and is responsible for a

44.87% yield loss in brinjal. The root knot nematode produces galls on the roots of many vegetables, pulses, some fruit crops, tobacco and ornamental crops and causes severe losses (Kapoor et al., 2012).

2.5.1. Culture preparation

Fresh egg masses of *M. incognita* were collected from stock culture and maintained on tomato (*Lycopersicum esculentum*) root tissues and kept in water for egg hatching. The eggs suspension was poured on a cotton wool filter paper and incubated at $28 \pm 2\,°C$ to obtain freshly hatched juveniles. Juveniles collected within 48 h were used for screening the nematicidal activity of VDDAP.

2.5.2. Mortality test

VDDAP was initially dissolved in DMSO and then in distilled water to make dilutions of 250, 150 and 50 $\mu g\,mL^{-1}$. Experiments were performed under laboratory conditions at $28 \pm 2\,°C$. About 100 freshly hatched second stage juveniles were suspended in 5 mL of each diluted compound and incubated. Distilled water with nematode larvae has been employed as the control. The dead nematodes were observed under an inverted binocular microscope. After an incubation of 24 and 48 h, percentage mortality was calculated. Nematodes were considered dead, if they do not move when probed with a fine needle (Cayrol et al., 1989).

2.6. Agarose gel electrophoresis

5 μL of λDNA was added to 2 μL of each sample (for $-ve$ control no sample is added, for $+ve$ control 2 μL $FeSO_4$ and VDDAP) seperately in eppendorf tubes. The contents were incubated at $37\,°C$ for 1 h and then 10 μL of enzyme buffer, 1 μL of Hind III enzyme and 13 μL of deionized water were added, incubated at $37\,°C$ for 3 h. The contents of the wells were mixed with bromophenol dye and separated through electrophoresis. Gel electrophoresis was performed at constant voltage (70 V). Bands were visualized by viewing the gel under UV light and photographed.

2.7. Anticancer activity

The cell lines were cultured in RPMI 1640 medium, supplemented with 10% fetal bovine serum (FBS) and 2 mM L-glutamine at $37\,°C$ in a humidified atmosphere containing 5% CO_2. About 5×10^3 cells/well was seeded in 96-well micro titer plate using a culture medium. After 24 h, the new medium with VDDAP in the concentration of 10, 20, 40 and 80 $\mu g\,mL^{-1}$ was added to respective wells and incubated for 48 h. After incubation the sulforhodamine B assay was performed.

2.7.1. Sulforhodamine B (SRB) assay

The cytotoxicity of VDDAP was assessed using a cell death assay based on detection of cells by sulforhodamine B (SRB), a stain specific for proteins. The cells were inoculated into 96-well micro titer plates in 90 μL at plating densities at a density of 5×10^3 cells per well depending on the doubling time of individual cell lines. After cell inoculation, the micro titer plates were incubated for 24 h prior to the addition of standard. After 24 h, one plate of each cell line was fixed *in situ* with trichloroaceticacid (TCA) to represent a measurement of the cell population for each cell line at the time of drug addition. Experimental drugs were solubilized in appropriate solvent by 400-fold in the desired final maximum test concentration and stored frozen prior to use. At the time of drug addition, an aliquot of frozen concentrate was thawed and diluted to 10 times the desired final maximum test concentration with complete medium containing test article at a concentration of 10^{-3}. Additionally three, 10-fold serial dilutions were made to provide a total of four drug concentrations plus control. Aliquots of 10 μL of these different drug dilutions were added to the appropriate micro titer wells already containing 90 μL of medium, resulting in the required final drug concentration. After the addition of compounds, plates were incubated for 48 h and the assay was terminated by the addition of cold TCA. Cells were fixed *in situ* by the gentle addition of 50 μL of cold 30% (w/v) TCA (final concentration, 10% TCA) and incubated for 60 min at $4\,°C$. Sulforhodamine B (SRB) solution (50 μL) at 0.4% (w/v) in 1% acetic acid has been added to each well and the plates were incubated for 20 min at room temperature. Bound stain was subsequently eluted with 10 mM trizma base and the absorbance was read on an Elisa plate reader at a wavelength of 540 nm with 690 nm reference wavelength. Percentage growth was calculated on a plate by plate basis for test wells relative to control wells. All experiments were repeated for a minimum of three times with each experiment done in four replicates. Adriamycin was served as the positive control compound in the cytotoxic assay.

3. Results and discussion

3.1. Powder XRD

The powder X-ray diffraction pattern (Fig. 1) of VDDAP shows peaks at 2θ of $5.5°$, $8.1°$, $10.8°$, $13.5°$, $21.2°$, $22.2°$ and the corresponding d-spacing's are 15.9, 10.8, 8.1, 6.5, 4.1, 3.9 . The peaks at 2θ of $21.2°$, $13.5°$, $22.2°$ indicate the presence of vanadium ions (Xue et al., 2010) of $VOPO_4$ phases (Pillai and Sahle-Demessie, 2004; Rownaghi et al., 2009) and hydrated $VOPO_4$ phases ($VOHPO_4 \cdot H_2O$) predominantly in the V^{4+} state with a small amount of V^{5+} species in VDDAP (Guan et al., 2008). Peak at $13.5°$ corresponds to the presence
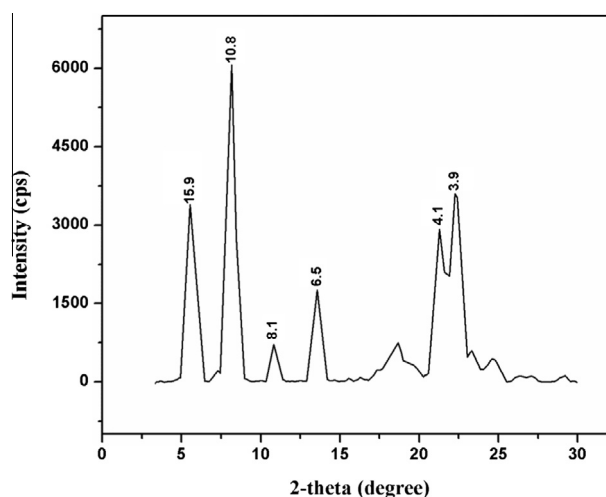

Figure 1   Powder X-ray diffraction pattern of VDDAP.

of hydrated $VOPO_4$ phases ($VOHPO_4.H_2O$). The crystallite size of the VDDAP was calculated by employing the Scherer's equation.

$$D = \frac{0.9\lambda}{\beta \cos \theta} \qquad (1)$$

where D represents the mean grain size, λ is the wavelength of X-ray radiation, β is the full width at half the maximum height of the peak and θ represents the diffraction angle. The average crystallite size of VDDAP was found to be 2.09 nm.

3.2. SEM-EDAX

The scanning electron micrograph (Fig. 2) of VDDAP synthesized using dodecylamine and vanadyl acetylacetonate shows that the particles have a fibrous morphology with homogenous phase. The energy dispersive X-ray analysis (Fig. 3) shows the distribution of the constituent elements O, P, N and V in the synthesized material.

3.3. FT-IR spectra

Fourier transform infrared spectrum (Fig. 4) of VDDAP shows a peak at 540 cm^{-1} associated with the V–O–V rotational vibrations. The small edge at 2920 cm^{-1} and the peak at 1475 cm^{-1} correspond to the asymmetric stretching and bending vibrations of methylene groups (–CH$_2$) of the alkyl group. The peak at approximately 1220–1080 cm^{-1} corresponds to the C–N stretching vibration. The peaks at 1085 cm^{-1} and 1171 cm^{-1} are due to the asymmetric stretching and anti-symmetric stretching of the P–O bond, respectively (Borah and Datta, 2010). The band at 1240 cm^{-1} can be ascribed to the asymmetric stretching vibration mode of the P–O bond (Nagaraju et al., 2008). The peaks in the range of 850–980 cm^{-1} are attributed to the stretching frequency of the –V=O bond in VDDAP (Nguyen-Phan et al., 2011). The peak at 889 cm^{-1} corresponds to the presence of condensed P–N units in VDDAP. The absence of bands at 1580 cm^{-1} and 1540 cm^{-1}, which are characteristic of the N-H bending vibrations of the NH$_3^+$ group, indicates that no protonation of amine has taken place (Datta et al., 2005). The structure of VDDAP was found to possess vanadium phosphate layers in which the amine molecules interact with the vanadium and phosphate to form an open-framework sandwiched polymeric material (Fig. 5).
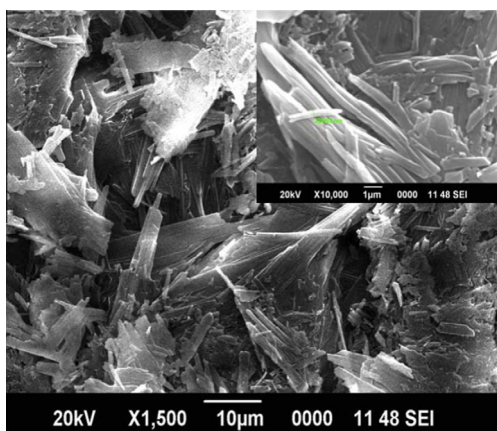

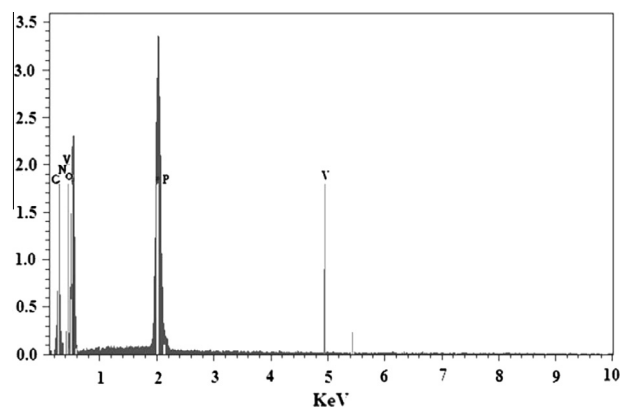**Figure 2** Scanning electron micrograph of VDDAP.

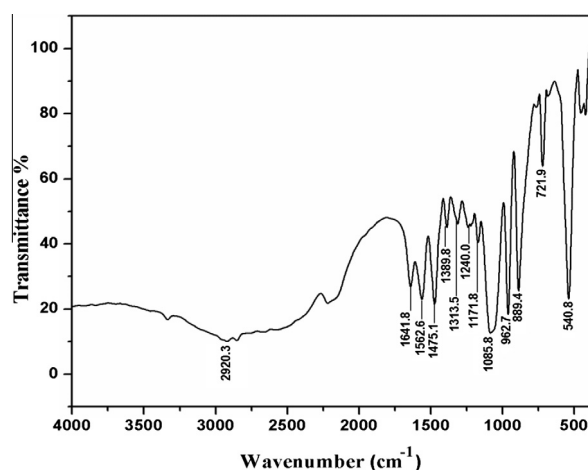**Figure 3** Energy dispersive X-ray analysis of VDDAP.

Figure 4 Fourier transform infrared spectrum of VDDAP.

3.4. Raman spectra

The dispersive Raman spectrum (Fig. 6) of VDDAP shows a small peak at 880 cm^{-1} corresponding to the presence of VOH-PO$_4$.H$_2$O (Guliants et al., 1996) while the band at 1050 cm^{-1} is assigned to the strong V–O–P band of the VOPO$_4$ phase in VDDAP (Went et al., 1990; Wu et al., 2010). The band near to 945 cm^{-1} corresponds to the symmetric stretching vibration of the phosphate tetrahedron of the VOPO$_4$ phase in VDDAP (Beneš et al., 2006).

3.5. UV–Vis DRS spectra

The UV–Vis diffused reflectance spectra (Fig. 7) of VDDAP shows a band at 250 nm due to the VO^{2+} species present in the tetrahedral coordination. The band at 300–320 nm favors high dispersion of V^{5+} ions in the tetrahedral environment (Murgia et al., 2006; Wang et al., 2011). The UV–Vis diffuse reflectance spectrum indicates that V^{4+} and V^{5+} ions are coexistent in VDDAP. The presence of a broad peak at 410–460 nm is due to the charge transfer transitions of the V^{5+} species (V=O) in square pyramidal geometry.
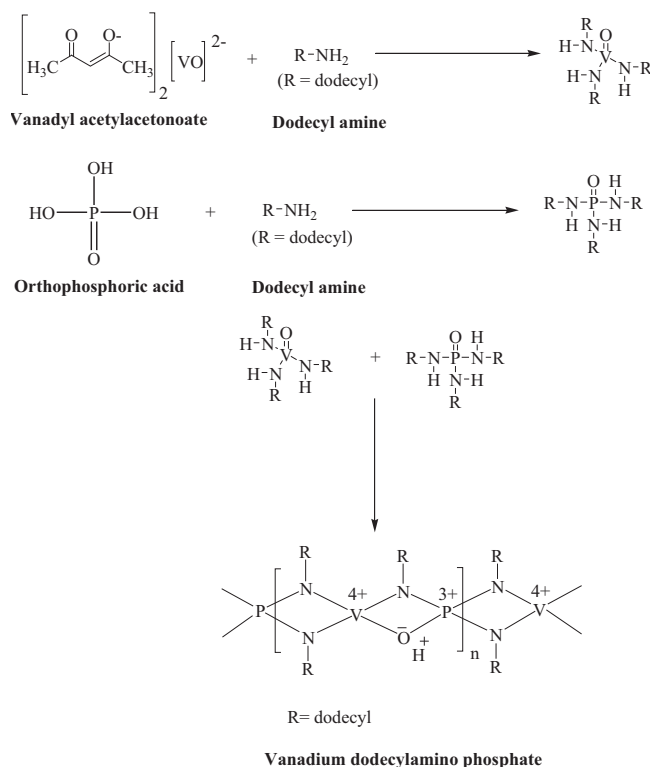
Figure 5 Mechanism proposed for the formation of VDDAP.

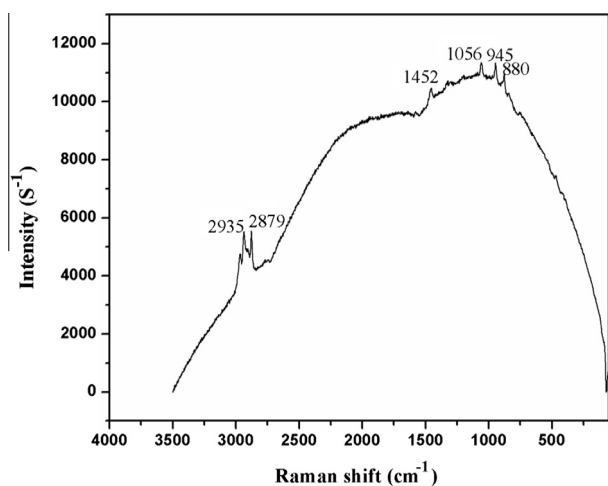**Figure 7** UltraViolet–Visible diffuse reflectance spectrum of VDDAP.

Figure 6 Dispersive Raman spectrum of VDDAP.
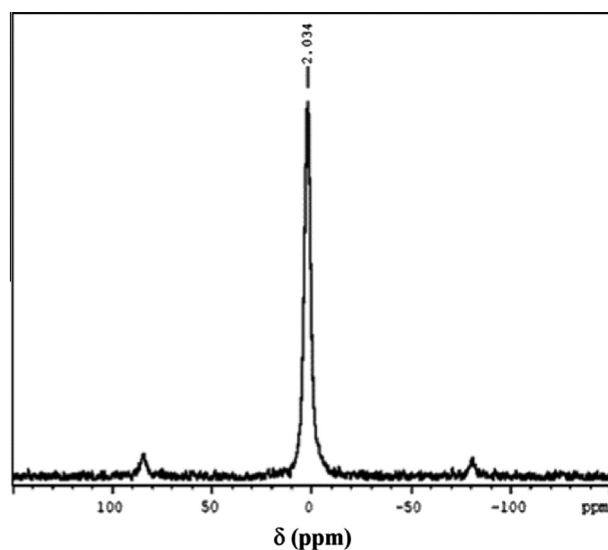
Figure 8 ^{31}P MAS NMR spectrum of VDDAP.

3.6. ^{31}P MAS NMR

The solid state ^{31}P MAS NMR spectrum (Fig. 8) of VDDAP shows a sharp signal centered at $\delta = 2.034$ ppm. The signal corresponds to the phosphorous atoms of the phosphate linkage. The ^{31}P MAS NMR signals in the δ range from –22 to 4 ppm correspond to the phosphorous atoms of the VOPO$_4$ phases. Only one resonance peak in the framework is a clear indicator that all the phosphorous atoms are equivalent in VDDAP (Bartley et al., 2001).
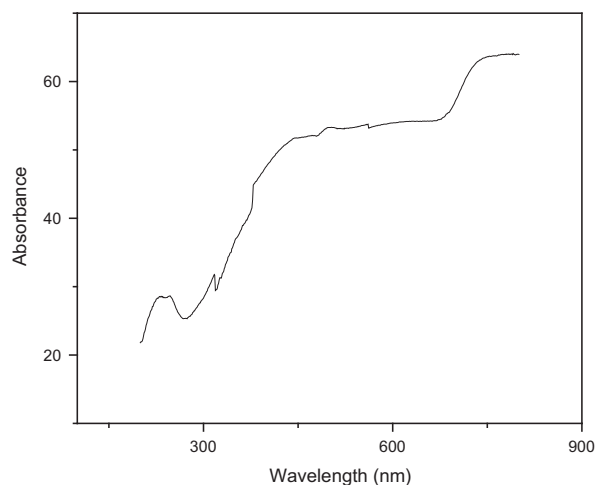
3.7. ^{13}C MAS NMR

The ^{13}C MAS NMR spectrum (Fig. 9) of VDDAP shows that the ^{13}C chemical shift in the δ range of 32–34 ppm due to the alkyl chains of interior methylene carbons in trans conformation (Dasgupta et al., 2002). The peak at $\delta = 14$ ppm is due to the interaction of the terminal methyl group of dodecylamine with the VPO matrix. The peaks at $\delta = 42.8$ and $\delta = 39.4$ ppm corresponds to the carbon (C$_1$) adjacent to the amine head group and the carbon (C$_2$) next to it respectively, indicating the strong interaction of the amine head group with the vanadium phosphate matrix (Dasgupta et al., 2004).

3.8. Antimicrobial activity

The antimicrobial activity of VDDAP was evaluated against bacterial species *S. aureus, B. subtilis, P. fluorescens, E. coli,*

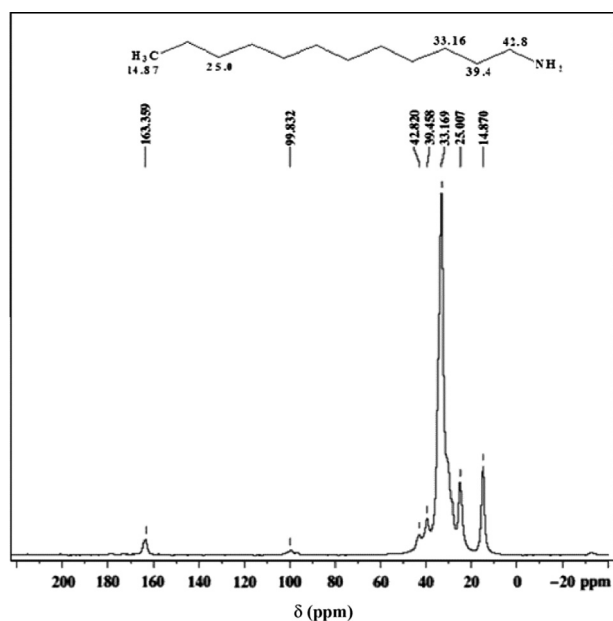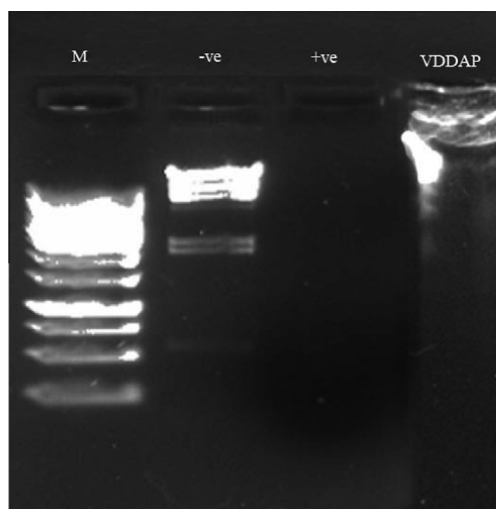**Figure 9** ^{13}C MAS NMR spectrum of VDDAP.

Figure 10 Gel electrophoresis diagram for DNA cleavage studies of λDNA by VDDAP in a buffer at 37 °C: lane, M = λDNA/EcoRI + Hind III enzyme, lane −ve = λDNA + Hind-III enzyme + without VDDAP, lane + -ve = λDNA + Hind-III enzyme + FeSO₄, lane VDDAP = λD-NA + Hind-III enzyme + VDDAP.

P. vulgaris and fungal species *C. albicans*. The results summarized in Table 1, are compared with those of the standard drug ampicillin for bacteria and clotrimazole for fungi. VDDAP displayed good anti-bacterial values against the Gram-positive strains. VDDAP inhibits the growth of bacteria and most of the MIC values were found in between 16 and 26 μg mL^{-1}. VDDAP shows the maximum anti-bacterial activity against *S. aureus* (Gram-positive) strain with an MIC value of 16 μg mL^{-1} and least against *P. fluorescens* (Gram-negative) bacteria with an MIC value of 26 μg mL^{-1} respectively. The MIC value against *E. coli* was found to be 20 μg mL^{-1}. The anti-fungal activity of VDDAP against *C. albicans* shows an MIC value of 18 μg mL^{-1}. Antimicrobial activity depends on the properties of amine side chains (Bonilla and García, 2012). Increase in the alkyl chain length of amine increases the hydrophobic interaction compatible with the lipid bilayer of the cell wall and in turn increases the antimicrobial activity (Sauvet et al., 2000). The dodecylamine in VDDAP provides a hydrophobic segment compatible with the bilayer of the outer cell wall and in turn increases the antimicrobial activity.

3.9. Nematicidal activity

The results of nematicidal activity of VDDAP on *M. incognita* are given in Table 2. From the results the highest nematicidal activity was observed at high concentrations and the activity was found to increase with increase in incubation time. It was found that the percentage mortality was increased from 54% to 66% with an increase in concentration from 150 to 250 μg mL^{-1} in a 48 h incubation time.

3.10. DNA cleavage studies

Gel electrophoresis experiment using λDNA was performed with the VDDAP. Fig. 10 shows the gel electrophoresis result. The DNA cleavage activity of VDDAP was evaluated by the conversion of super coiled DNA (SC, form I) to nicked circular (NC form II) or linear DNA (LC form III). It was found that the lane VDDAP clearly shows the absence of marker bands and without using any oxidant, VDDAP shows good DNA cleavage activity (Fig. 10, lane VDDAP). We also carried control experiments (−ve and +ve) under similar experimental conditions. In the Fig. 10 the −ve control (λDNA + without VDDAP) does not show cleavage activity and +ve control (λDNA + FeSO₄) shows a good DNA cleavage activity.

3.11. Cytotoxicity

The results of cytotoxicity of VDDAP are shown in Table 3. It was found that the VDDAP shows a dose dependent anti

Table 1 MIC in μg mL^{-1} for antimicrobial activity of VDDAP.

Compound	Gram-positive bacteria		Gram-negative bacteria			Fungus
	Staphylococcus aureus	*Bacillus subtilis*	*Proteus vulgaris*	*Pseudomonas fluorescens*	*Escherichia coli*	*Candida albicans*
VDDAP	16	18	22	26	20	18
Ampicillin	12	14	16	16	16	–
Clotrimazole	–	–	–	–	–	10

Note: (−) sign indicates no inhibition.

Table 2 Nematicidal activity (% mortality) on *Meloidogyne incognita* at different time intervals. % Mortality observed against different concentrations.

Compound	After 24 h			After 48 h		
Concentration µg mL^{-1}	250 µg mL^{-1}	150 µg mL^{-1}	50 µg mL^{-1}	250 µg mL^{-1}	150 µg mL^{-1}	50 µg mL^{-1}
VDDAP	35	20	10	66	54	33

Table 3 Cytotoxicity studies of VDDAP on HL60, HeLa and MCF7 cancer cell lines using sulforhodamine B assay.

Cell lines	LC50		TGI		GI50	
	VDDAP	Adriamycin	VDDAP	Adriamycin	VDDAP	Adriamycin
HL60	> 80	> 80	47.8	43.8	11.6	< 10
HeLa	60.5	28.8	42.9	< 10	25.4	< 10
MCF7	> 80	55.2	62.7	15.8	29.1	< 10

Adriamycin was used as positive control drug.
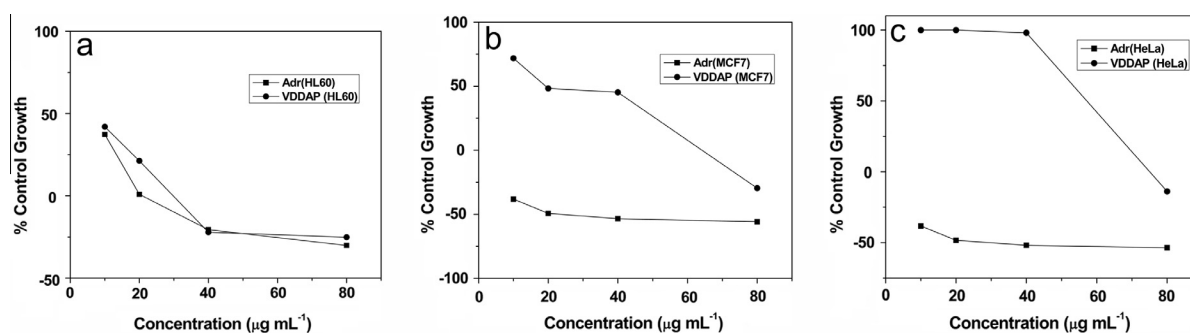
Figure 11 Cytotoxicity studies of (a) VDDAP on HL60 against Adriamycin (HL60) (b) VDDAP on MCF7 against Adriamycin (MCF7) (c) VDDAP on HeLa against Adriamycin (HeLa).

proliferative effect toward cancer cell lines. According to the dose response curves, the VDDAP had strong inhibitory effect on cancer cell lines. Estimations based on GI50 values show that VDDAP exhibits excellent anticancer activity on HL60 cells (GI50 = 11.6 µg mL^{-1}) at 40 and 80 µg mL^{-1} concentrations and good activity on MCF7 (GI50 = 29.1 µg mL^{-1}) and HeLa (GI50 = 25.4 µg mL^{-1}) cell lines at 80 µg mL^{-1} concentration levels (Fig. 11). Interestingly, VDDAP shows a significant and interesting cytotoxicity on HL60 than HeLa and MCF7 cell lines respectively and suggests the potential for future development of VDDAP as a cell type specific inhibitor.

4. Conclusions

This paper demonstrates, the synthesis of a novel VDDAP at ambient temperature by employing a vanadium precursor in the presence of phosphate using organic amine as the template. The powder XRD data suggest the presence of VOPO$_4$ and hydrated VOPO$_4$ phases in the framework of the material. Fibrous nature of the synthesized material has been confirmed from the SEM micrograph. The presence of –V=O and –V–O–P– bonds in the framework was confirmed by the presence of the corresponding vibration bands of the infrared and Raman spectra. The coexistence of V^{4+} and V^{5+} in the framework was suggested from the UV–Vis DRS studies. The ^{31}P MAS NMR spectrum revealed the phosphorous atoms to be of the VOPO$_4$ phases. ^{13}C suggests the interaction of an amino group with the vanadium phosphate matrix. The material exhibits a good antimicrobial activity against Gram-positive strains and nematicidal activity at high concentrations. VDDAP promotes the cleavage of λDNA and also explored for *in vitro* cytotoxicity on cancer cell lines observing that the material is active on all cell lines. However, VDDAP shows good cytotoxicity on HL60 with high GI50 value than HeLa and MCF7 cell lines. VDDAP also exhibits a dose dependent cytotoxic effect on cancer cell lines. In conclusion, the material VDDAP represents a potentially active novel drug with respect to its antimicrobial, DNA binding and a promising strategy in the treatment of leukemia.

References

Bartley, J.K., Kiely, C.J., Wells, R.P.K., Hutchings, G.J., 2001. Catal. Lett. 72, 99–105.

Beneš, L., Melánová, K., Zima, V., Trchová, M., Čapková, P., Koudelka, B., 2006. J. Phys. Chem. Solids. 67, 956–960.

Benítez, J., Becco, L., Correia, I., Leal, S.M., Guiset, H., Pessoa, J.C., Lorenzo, J., Tanco, S., Escobar, P., Moreno, V., Garat, B., Gambino, D., 2011. J. Inorg. Biochem. 105, 303–312.

Bishayee, A., Waghray, A., Patel, M.A., Chatterjee, M., 2010. Cancer Lett. 294, 1–12.

Bonilla, A.M., García, M.F., 2012. Prog. Polym. Sci. 37, 281–339.

Borah, P., Datta, A., 2010. Appl. Catal., A: General 376, 19–24.

Cayrol, J., Djian, C., Pijarowski, L., 1989. Rev. Nematologie 12, 331–336.

Chasteen, N.D., Clarke, M.J., Goodenough, J.B., Hemmerich, P., Ibers, J.A., Joergensen, C.K., Neilands, J.B., Reinen, D., Weiss, R., Williams, R.J.P., 1983. Structure and Bonding. Springer-Verlag, Berlin, Heidelberg, New York, 53, 105–138.

Dasgupta, S., Agarwal, M., Datta, A., 2002. J. Mater. Chem. 12, 162–164.

Dasgupta, S., Agarwal, M., Datta, A., 2004. Microp. Mesop. Mater. 67, 229–234.

Datta, A., Dasgupta, S., Agarwal, M., Ray, S.S., 2005. Microp. Mesop. Mater. 83, 114–124.

Guan, J., Xu, H., Jing, S., Wu, S., Ma, Y., Shao, Y., Kan, Q., 2008. Catal. Commun. 10, 276–280.

Guliants, V.V., Benziger, J.B., Sundaresan, S., Wachs, I.E., Jehng, J.-M., Roberts, J.E., 1996. Catal. Today 28, 275–295.

Heater, S.J., Carrano, M.W., Rains, D., Walter, R.B., Ji, D., Yan, Q., Czernuszewicz, R.S., Carrano, C.J., 2000. Inorg. Chem. 39, 3881–3889.

Kapoor, P., Singh, R.V., Fahmi, N., 2012. J. Coord. Chem. 65, 262–277.

Maia, P.I.d.S., Pavan, F.R., Leite, C.Q.F., Lemos, S.S., de Sousa, G.F., Batista, A.A., Nascimento, O.R., Ellena, J., Castellano, E.E., Niquet, E., Deflon, V.M., 2009. Polyhedron, 28, 398–406.

Morinville, A., Maysinger, D., Shaver, A., 1998. Trends Pharmacol. Sci. 19, 452–460.

Murgia, V., Torres, E.M.F., Gottifredi, J.C., Sham, E.L., 2006. Appl. Catal. 312, 134–143.

Nagaraju, P., Lingaiah, N., Prasad, P.S.S., Kalevaru, V.N., Martin, A., 2008. Catal. Commun. 9, 2449–2454.

Nguyen-Phan, T.-D., Song, M.B., Yun, H., Kim, E.J., Oh, E.-S., Shin, E.W., 2011. Appl. Surf. Sci. 257, 2024–2031.

Ott, I., Gust, R., 2007. Arch. Pharm. (Weinheim) 340, 117–126.

Pillai, U.R., Sahle-Demessie, E., 2004. Appl. Catal. A. 276, 139–144.

Rajini, A., Nookaraju, M., Selvaraj, K., Reddy, I.A.K., Narayanan, V., 2013. Mat. Res. 16, 181–189.

Reddy, P.P., Khan, R.M., 1991. Curr. Nematol. 2, 115–116.

Rownaghi, A.A., Taufiq Yap, Y.H., Rezaei, F., 2009. Chem. Eng. J. 155, 514–522.

Sauvet, G., Dupont, S., Kazmierski, K., Chojnowski, J., 2000. J. Appl. Polym. Sci. 75, 1005–1012.

Shahzadi, S., Ali, S., Sharma, S.K., Qanungo, K., 2010. J. Iran. Chem. Soc. 7, 419–427.

Shi, X., Jiang, H., Mao, Y., Ye, J., Saffiotti, U., 1996. Toxicology 106, 27–38.

Thompson, K.H., McNeil, J.H., Orvig, C., 1999. Chem. Rev. 99, 2561–2572.

Verquin, G., Fontaine, G., Bria, M., Zhilinskaya, E., Abi-Aad, E., Aboukais, A., Baldeyrou, B., Bailly, C., Bernier, J.L., 2004. J. Biol. Inorg. Chem. 9, 345–353.

Wang, C.-T., Chen, M.-T., Lai, D.-L., 2011. Appl. Surf. Sci. 257, 5109–5114.

Went, G.T., Oyama, S.T., Bell, A.T., 1990. J. Phys. Chem. 94, 4240–4246.

Wu, Z.L., Dai, S., Overbury, S.H., 2010. J. Phys. Chem. C 114, 412–422.

Xue, M., Chen, H., Zhang, H., Auroux, A., Shen, J., 2010. Appl. Catal. 379, 7–14.